Mobility modulation in vertical transport of hot electrons in multiquantum-well structures

S. Maimon

Department of Electrical Engineering, Technicion—Israel Institute of Technology, Haifa, Israel

S. E. Schacham,[1]

Department of Electrical and Electronic Engineering, College of Judea and Samaria, Ariel, Israel

G. Bahir, E. Finkman, and D. Ritter

Department of Electrical Engineering, Technicion—Israel Institute of Technology, Haifa, Israel

(Received 25 March 1996)

Perpendicular mobility of photoexcited electrons in multi-quantum-well (MQW) structures, is modulated by photon energy. The period equals the energy of optical phonons. This theoretical prediction was verified experimentally in InPIn$_x$Ga$_{1-x}$As MQW's, proving that in MQW's the average photocarrier energy is higher than thermal. In bulk material this effect is absent since the thermalization rate is faster than recombination. Monte Carlo simulations render an excellent fit to measured data. A model for the dominant unscreened ionized impurity scattering is presented, upgrading the Conwell-Weskopf theory. [S0163-1829(96)02432-0]

There has been a great deal of interest recently in studying hot-carrier transport above the energy barriers in multiquantum-well (MQW) heterostructures, as well as electron recapture into quantum wells.[1–8] Investigation of the transport properties of photoexcited electrons in MQW structures is of great importance in understanding the physical processes in various advanced electronic devices. In particular, vertical transport of electrons is crucial in structures such as quantum-well infrared photodetectors (QWIP's), heterostructure bipolar transistors, semiconductor lasers, and hot-electron transistors. QWIP's have the potential of replacing conventional narrow-gap detectors as sensing elements for the infrared region. Presently, the performance of state-of-the-art QWIP's is inferior to that of conventional systems, pending further research. While the optical properties of these devices are quite well understood, the electronic processes are less studied. Transport of electrons excited to the barriers in MQW structures is different from that in bulk material, due to the presence of the wells. This issue received little attention so far.

In this paper the mobility of optically excited carriers traveling perpendicular to the epitaxial layers in QWIP structures is investigated. The various scattering mechanisms affecting the mobility as a function of excitation energy are analyzed. One of the most interesting phenomena is that, in MQW's, the average energy of the optically excited carriers can be considerably larger than that of thermally excited carriers. This is due to the fact that while in bulk semiconductors the thermalization time is orders of magnitude shorter than the lifetime, here the thermalization time is longer than the electron recapture time. Therefore, thermalization is negligible, and, unlike the situation in bulk semiconductors, the electrons maintain the kinetic energy obtained by photoexcitation. The dominant scattering mechanism is due to unscreened ionized impurities in the barrier, for which the mobility increases with increased energy. Thus it is expected that, as the excitation energy increases, the perpendicular mobility increases. This holds as long as the kinetic energy

of the carriers above the barriers is smaller than that of longitudinal-optical (LO) phonons $\hbar\omega_{LO}$. Once the kinetic energy reaches $\hbar\omega_{LO}$, an abrupt drop in the mobility should occur following the emission of a phonon. The process should repeat itself for multiples of $\hbar\omega_{LO}$.

We verified our theoretical prediction experimentally on a lattice-matched InP/In$_x$Ga$_{1-x}$As MQW grown by metalorganic molecular-beam epitaxy. An n^+ In$_x$Ga$_{1-x}$As contact layer was grown on the InP substrate, followed by 20 periods of InP barriers and In$_x$Ga$_{1-x}$As well, concluded by another In$_x$Ga$_{1-x}$As contact layer. The well is 50 Å wide, with a donor concentration of 2×10^{17} cm^{-3}. The barrier is 570 Å wide, with an unintentional donor concentration of $2–3\times10^{11}\times10^{16}$ cm^{-3}. The combined doping in the well and barrier regions resulted in electron sheet concentration of $2–3$ cm^{-2} in the wells. The test device is a QWIP structure, with a 200×200-μm^2 mesa. The light was introduced via a wedge, to provide radiation with polarization necessary for intersubband absorption.[1]
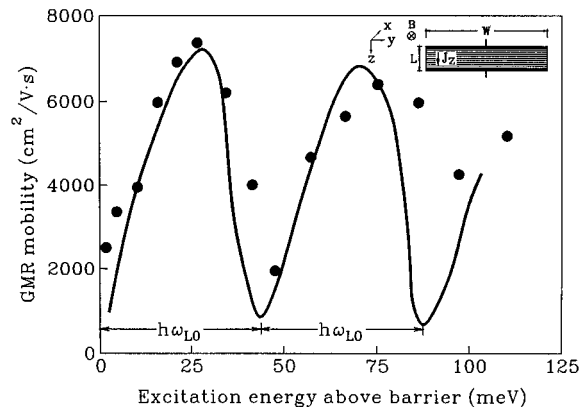
FIG. 1. Vertical mobility of photoexcited electrons in a InP/In$_x$Ga$_{1-x}$As MQW structure vs their initial energy above the barrier. The barrier is 160 meV higher than E_1. Circles—experiment; line—model simulation. Inset: GMR sample arrangement.

The carrier mobility as a function of excitation energy was measured using the photo geometrical magnetoresistance (GMR) method,[9,10] at a temperature of 13 K. The change in longitudinal resistivity in the z direction is measured as a function of the magnetic field B, applied along the x axis (see the inset in Fig. 1). In a conventional Hall measurement, a Hall electric field is developed along the sample width W, in the y direction, to exactly balance the Lorentz force on the carriers. A GMR sample is a thin plate with metallic contacts on the wide faces. The Hall field is shortened by the contacts, since the length L is much smaller than W. The Lorentz force is no longer compensated for and GMR's is observed, from which the mobility can be determined. Unlike physical magnetoresistance, in which the reduction in the longitudinal current is due to the presence of more than one type of carrier, here the effect is due to the geometrical boundary conditions. In optical GMR one measures the change in photoexcited current, $J_{ph}(B)$, under a constant applied electric field in the z direction. It was measured to decrease quadratically with the magnetic field. The GMR mobility is given by

$$\mu_{GMR} \equiv \left(\frac{1}{B}\right)\left(\frac{J_{ph}(0)}{J_{ph}(B)} - 1\right)^{1/2} = \left(\frac{1}{B}\right)\left(\frac{\nu_{d,ph}(0)}{\nu_{d,ph}(B)} - 1\right)^{1/2}$$

$$\cong \mu_{cond}, \tag{1}$$

where $\nu_{d,ph}$ is the drift velocity of the photoexcited carriers. For most common scattering mechanisms, it is almost identical to the conductivity mobility μ_{cond}.

The GMR mobility was recorded as a function of IR energy by using a circular variable interference filter. This enables the determination of the initial kinetic energy of excited electrons above the barrier E_b. Experimental results, presented in Fig. 1, show a clear mobility modulation with a period of 43–44 meV, which corresponds to $\hbar\omega_{LO}$ in InP. Since absorption decreases at high energies, only two periods of modulation could be measured.

The actual drop in mobility is not abrupt due to broadening of the energy of free electrons, caused mainly by three effects: (i) the range of energies of electrons in the well, between the confined level E_1 and the Fermi energy; (ii) the kinetic energy due to the applied electric field; and (iii) variations in E_1 caused by fluctuations in the well width. Detailed analysis of these processes is given elsewhere.[11] To measure a meaningful spectrum, it is essential that the total broadening is substantially smaller than the excitation energy above the barrier. Thus the structure was designed with a low carrier concentration, and low electric fields were employed. The measurements presented in Fig. 1 were taken at a field of 500 V/cm. Under these conditions the dominant broadening mechanism is due to the applied electric field. The calculated broadening is $\Delta E \approx 16$ meV. The signal was found to be linear both with electric field and with optical excitation intensity. In an experiment performed at 4000 V/cm the modulation in mobility was indeed absent, due to broadening.

Electrons contribute to the photocurrent only when they are above the barriers. Since their mobility is energy dependent, energy relaxation is analyzed. Momentum and energy scattering mechanisms are relevant only if the associated relaxation times are not much longer than the effective lifetime. Three time constants characterize the electron transport

above the barriers: energy relaxation time τ_E; momentum relaxation time τ_m; and recapture time into the well τ_c, which is equivalent to lifetime in bulk semiconductors. The expressions for energy and momentum relaxation times due to deformation potential, piezoelectric and LO phonons are given in Ref. 12. The recapture time can be derived either from time-resolved photoluminescence[7,8] or from the gain of photodetectors.[6,9] For low electric fields this time is in the picosecond range in InP/In$_x$Ga$_{1-x}$As QWIP's.[7] Since only one confined energy level exists in our structure, τ_c is almost energy independent, as observed by Blom et al.,[8] in contrast to the situation in which a second shallow level is present.

In bulk III-V, for carriers with energy larger than $\hbar\omega_{LO}$, the relaxation time involving the emission of an LO phonon is extremely short, about 0.1 ps. In material with small impurity and electron concentrations, the thermalization of excited electrons with energy below $\hbar\omega_{LO}$ is dominated by acoustic phonon-scattering through deformation-potential and piezoelectric mechanisms, so τ_E is of the order of 100 ps, much shorter than the recombination time. For hot-electrons in a MQW structure, the transit time between wells is short (≈ 0.1 ps), and τ_c is a few ps. Thus thermalization rates due to deformation-potential and piezoelectric mechanisms are now negligible, and the dominating energy relaxation time at low excitation energies is τ_c. Electrons which are excited with a kinetic energy $E_b > \hbar\omega_{LO}$ perform a Brownian motion with an energy of $E_b - \hbar\omega_{LO}$, following the rapid release of an optical phonon. If $E_b < \hbar\omega_{LO}$ the Brownian motion continues with E_b until they are captured at one of the wells. This holds only at low electric fields, at which the incremental energy acquired due to the field between excitation and capture is much less than $\hbar\omega_{LO}$.

At 13 K, the free-electron concentration in the barrier, due either to doping or photoexcitation, is very low, below 10^8 cm^{-3}. Thus electron-electron scattering within the barrier is negligible. In the well, both electron-electron and electron-plasmon scattering are negligible in our structure, for two reasons. First, the concentration of electrons is low. Second, the large collision damping associated with the low mobility of electrons within the well (~ 1000 cm^2/V s). A detailed calculation by the random-phase approximation method shows an energy relaxation time of more than 10 ps due to these processes.

The momentum is affected by LO scattering only if the carrier kinetic energy is larger than $\hbar\omega_{LO}$. At low fields, the dominant momentum scattering process is due to ionized impurities in the barrier. These donors are not screened by electrons in that region, because of the low electron concentration. On the other hand, the ionized donors in the well are screened, and therefore their effect on the momentum is less significant.

The conventional analysis of momentum relaxation due to unscreened ionized impurities is based on the model of Conwell and Weisskopf (CW).[13] This model uses the Born approximation, which is valid for high energies only. It also assumes a minimal deflection angle which is derived from classical mechanics (Rutherford theory). The latter assumption is needed in order to overcome the divergence of scattering rates. Monte Carlo (MC) simulations with this model, with the nominal donor concentration, predict mobility values which are 3–4 times higher than experimental results,

indicating a scattering rate lower than expected. An adequate mobility could be obtained by increasing doping concentrations to unreasonable levels. A more suitable model for low-energy carriers is required. In our work the model of CW is modified by replacing the minimal deflection angle by a maximum range of the unscreened potential (the maximum impact parameter of CW). This allows integrating the rate over all scattering angles, including the small ones, which are not included in CW. The range is taken as half the average distance between scatterers, $b = N_D^{-1/3}/2$, where N_D is the donor concentration. A comparison is performed between the momentum relaxation time calculated using three models: CW, our model by the quantum-mechanics phase shift (QMPS) technique,[14] and ours by the Born approximation.

Using the QMPS, the scattering cross section was derived for the first 60 orders in the phase shift. The momentum scattering cross section is given by[15]

$$\sigma_m(k) = \frac{4\pi}{k^2} \sum_{l=0}^{\infty} (l+1)\sin^2(\delta_l - \delta_{l+1}), \qquad (2)$$

where k is the wave vector. The phase shift of the l order, δ_l, is computed numerically by solving the Schrödinger equation. The momentum relaxation time is given by[15] $\tau_{m(\text{phase shift})} = (N_D \nu \sigma_m)^{-1}$, where ν is the electron velocity.

In the Born approximation, transition rates due to scattering from a single scatterer are given by

$$S(k,k') = \frac{2\pi}{\hbar} \left(\frac{q^2}{\Omega \varepsilon_s \varepsilon_0} \right)^2 \left(\frac{1 - \cos(\Delta k b)}{\Delta k^2} \right)^2 \delta(E - E'), \qquad (3)$$

where $\varepsilon_s \varepsilon_0$ is the static dielectric constant, Ω is the volume, Δk is $|\mathbf{k} - \mathbf{k}'| = 2\mathbf{k}\sin(\alpha/2)$, and α is the scattering angle. The resulting momentum relaxation time is

$$\tau_{m(\text{Born})}(k) = \left\{ \frac{N_D}{2\pi} \left(\frac{q^2}{\varepsilon_s \varepsilon_0} \right)^2 \frac{m^*}{\hbar^3} k \int_{-1}^{1} \frac{\left\{ 1 - \cos\left[2k\sin\left(\frac{\alpha}{2}\right)b \right] \right\}^2}{\left[2k\sin\left(\frac{\alpha}{2}\right) \right]^4} (1-\cos\alpha) d(\cos\alpha) \right\}^{-1}. \qquad (4)$$

The integrand is finite for $\alpha \to 0$ and the integral converges.

Figure 2 shows the calculated momentum relaxation time for the three models. For low energies, below $\hbar \omega_{\text{LO}}$, the relaxation time derived from the QMPS for our model is shorter by a factor of 2–3 from that of CW, while at larger energies the two models converge, as expected. In the intermediate range, above 15 meV, our Born approximation is almost identical to the QMPS results. In the relevant energy range, above a few meV, τ_m increases with energy. Its average value in the low-energy range is an order of magnitude smaller than the recapture time (2 ps), which justifies the assumption of Brownian motion. Since the present model does not impose the Rutherford restriction over the minimum
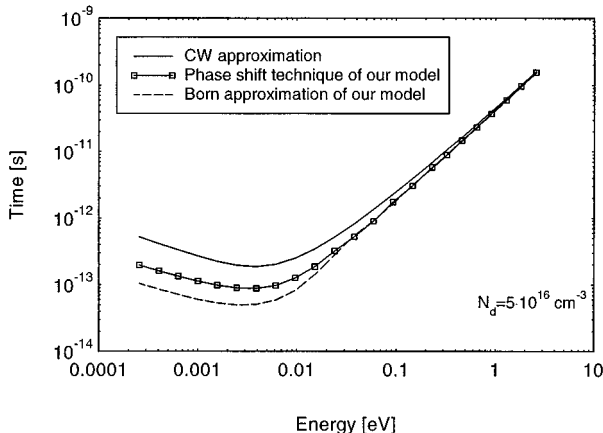
scattering angle, it should provide improved results in low concentration bulk material, for quantum effects of low-energy particles.

The mobility as a function of excitation energy was derived from a three-dimensional Monte Carlo simulation of the GMR experiment, as given in Eq. (1). The following assumptions were made: (a) The recapture time is 2 ps, and is energy independent.[8] (b) Only LO phonons and ionized impurity scattering were included. Piezoelectric, deformation potential, and electron-electron scattering were neglected due to their long relaxation times. (c) All carriers in the wells have zero momentum in the x-y plane. (d) The initial momentum of the particle before the first scattering event is either in the $+z$ or $-z$ direction, with a probability of 50%. (e) When an electron is recaptured, another carrier is generated, with energy E_b, so that the overall charge is conserved. (f) The effect of the magnetic field was included using the equation of motion following each scattering event.[16] (g) The effect of the contacts is negligible. (h) The sample is infinite in the xy plane, a necessary condition for GMR experiments.

For MC simulations we used our model for the ionized impurity scattering, while the scattering due to LO phonons was derived using Ref. 17. To ensure reliable results, 10 000 particles were taken for the simulations, for a duration of 50 ps, a time long enough to reach a steady state. With a field of 500 V/cm, the minimal drift velocity in the simulation is $\approx 10^6$ cm/s. For a thermal velocity of 2–3×10^7 cm/s, one scattering event does not give a significant perturbation on the ensemble averaged drift velocity. Hence the use of MC simulations is justified. The average drift velocity was calculated using

$$\nu_d(B) = \sum_{i=l}^{N} \nu_{z,i}(B)/N, \qquad (5)$$

FIG. 2. Calculated momentum relaxation time as predicted by three models: Conwell and Weisskopf; our model using the phase-shift technique; and our model using the Born approximation.
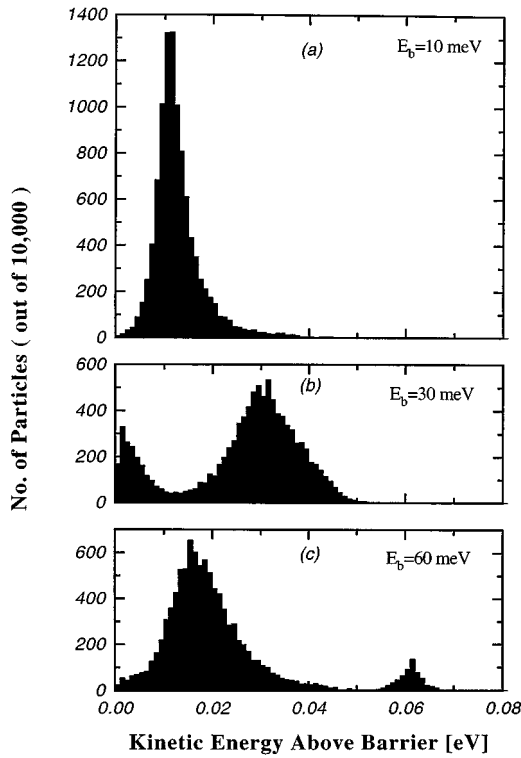
FIG. 3. Histograms describing the steady-state energy distribution of electrons, excited with three different initial kinetic energies above the barrier. (a) $E_b = 10$ meV. (b) $E_b = 30$ meV. (c) $E_b = 60$ meV. The only source of broadening in this Monte Carlo simulation is due to the electric field. Important: for such an electron distribution it is impossible to define a quasi-Fermi energy or hot-electron temperature.

where $\nu_{z,i}$ is the velocity of the i particle in the z direction, while N is the number of particles in the simulation. μ_{GMR} was derived by inserting ν_d, calculated with and without magnetic field, into Eq. (1). The variance in ν_d was found to be 10% for a single simulation. An average of 1000 simulations was taken to improve the variance to better than 1%,

enabling the determination of a GMR signal, typically of the order of 10–20 % for the maximum available field of 0.6 T. The drift velocity, calculated at fields of 500 and 250 V/cm, was found to be linear with the field.

The fundamental parameter in device performance is the conductivity mobility, which differs from the GMR mobility by the scattering factor r_{GMR}. To estimate this factor, the energy of the i particle, E_i, is derived from MC simulations, and introduced in $\tau_m(E_i)$ to render[18]

$$r_{GMR} = N \left[\sum_{i=1}^{N} \tau_m^3(E_i) \middle/ \left(\sum_{i=1}^{N} \tau_m(E_i) \right)^3 \right]^{1/2}.$$

This factor is found to be between 1 and 1.1, with minimal effect of the magnetic field.

The line in Fig. 1 shows the results of the simulation for the GMR mobility as a function of the initial kinetic energy, for an electric field of 500 V/cm. The doping concentration was taken as a parameter for fitting the measured data. The best fit was obtained for a donor concentration of 3.3×10^{16} cm^{-3}. The agreement between the experimental results and this simulation is very good.

The assumptions of zero momentum in the x-y plane and a single excited energy E_b [assumptions (c) and (e) above] imply neglecting broadening in energy due to fluctuations in the well width and due to the initial kinetic energy. Thus the only source of broadening in the MC simulations presented in Fig. 1 is due to the electric field. The good agreement with the experiment indicates the validity of these assumptions. Figure 3 shows the histograms of particles as a function of their kinetic energy at steady state, produced by the MC calculations. The broadening in the figure is due to the electric field only, which suffices to cause a significant broadening in carriers kinetic energy.

In conclusion, we have demonstrated that the low-field perpendicular mobility of hot-electrons above the energy barriers in MQW structures is modulated as a function of excitation energy, with a period of $\hbar\omega_{LO}$. The mobility spectrum fits the theoretical prediction based on unscreened ionized impurity scattering, for which a model was developed.

[1] B. F. Levine, J. Appl. Phys. **74**, R1 (1993).

[2] E. Rosencher *et al.*, IEEE Trans. Quantum Electron **30**, 2875 (1994).

[3] F. Luc *et al.*, Appl. Phys. Lett. **62**, 1143 (1993).

[4] *Thin Films*, edited by M. H. Francombe and J. L. Vossen (Academic, San Diego, 1995), Vol. 21.

[5] B. F. Levine *et al.*, Phys. Rev. Lett. **63**, 899 (1989).

[6] E. Rosencher *et al.*, Appl. Phys. Lett. **63**, 3312 (1993).

[7] R. Kersting *et al.*, Phys. Rev. B **46**, 1639 (1993).

[8] P. W. M. Blom *et al.*, Phys. Rev. B **47**, 2072 (1993).

[9] M. J. Kane *et al.*, J. Appl. Phys. **73**, 7966 (1993).

[10] A. Fraenkel *et al.*, J. Appl. Phys. **75**, 3536 (1994).

[11] S. Maimon *et al.* (unpublished).

[12] B. K. Ridley, *Quantum Processes in Semiconductors* (Clarendon, Oxford, 1988).

[13] E. Conwell and V. F. Weisskopf, Phys. Rev. **77**, 388 (1950).

[14] E. Merzbacher, *Quantum Mechanics* (Wiley, New York, 1961).

[15] L. E. Kay, and T. W. Tang, J. Appl. Phys. **70**, 1475 (1991).

[16] C. Jacoboni and L. Regianni, Rev. Mod. Phys. **55**, 645 (1983).

[17] W. Fawcett *et al.*, J. Phys. Chem. Solids **31**, 1963 (1970).

[18] D. C. Look and G. B. Norris, Solid-State Electron. **29**, 159 (1986).